Journal of Hazardous Materials 491 (2025) 137911

Contents lists available at ScienceDirect

Journal of Hazardous Materials

journal homepage: www.elsevier.com/locate/jhazmat

Distribution characteristics and transport processes of biodegradable microplastics in the Seto Inland Sea, Japan

Yu Bai [a], Xinyu Guo [b,*], Takashi Masaki [c], Takako Kikuchi [d], Tomoya Kataoka [b,e], Hirofumi Hinata [b,e,f,g], Xueting Zhao [a], Yaxian Li [a]

[a] Graduate School of Science and Engineering, Ehime University, 2-5 Bunkyo-Cho, Matsuyama, Ehime 790-8577, Japan
[b] Center for Marine Environmental Studies, Ehime University, 2-5 Bunkyo-Cho, Matsuyama, Ehime 790-8577, Japan
[c] Kureha Corporation, 16 Ochiai, Nishiki-machi, Iwaki, Fukushima 974-8686, Japan
[d] Chemicals Evaluation and Research Institute, 1600 Shimotakano, Sugito-machi, Kitakatsushika-gun, Saitama 345-0043, Japan
[e] Department of Engineering, Faculty of Engineering, Ehime University, 3 Bunkyo-Cho, Matsuyama, Ehime 790-8577, Japan
[f] South Ehime Fisheries Research Center, Ehime University, 1289-1, Funakoshi, Ainan, Ehime 798-4292, Japan
[g] Center for Disaster Mitigation Informatics Research, Ehime University, 3 Bunkyo-cho, Matsuyama, Ehime 790-8577, Japan

HIGHLIGHTS

- The fate and mass budget of biodegradable microplastics (MPs) are elucidated.
- MPs distribution and behavior varied in marine environments.
- The transport of MPs is simulated using a 3D hydrodynamic model.
- Settling velocity is a significant driver of the deposition and transport of MPs.
- The concentration of MPs in the sediment stabilizes with a degradation rate of $> 2.44\times10^{-3}$ d^{-1}.

GRAPHICAL ABSTRACT

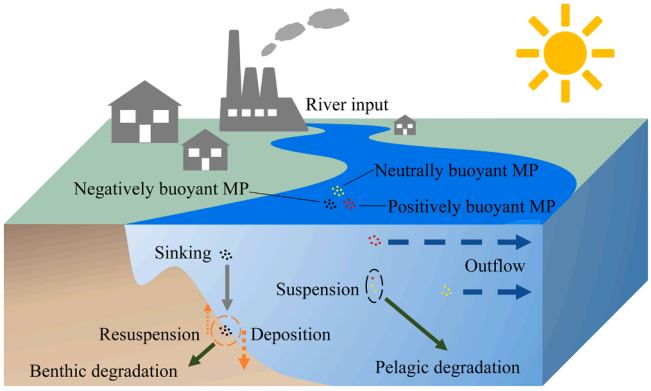

ARTICLE INFO

Keywords:
Microplastics
Spatiotemporal distribution
Settling velocity
Biodegradation
Seto Inland Sea

ABSTRACT

Microplastics (MPs) pollution is a prevalent environmental problem that affects ecosystems globally. Despite the growing research on the environmental effects of MPs, a significant research gap remains in understanding the differences of environmental behavior and distribution patterns between biodegradable MPs and traditional MPs. Using a three-dimensional hydrodynamic model and treating MPs as tracers with vertical velocity, this study simulated the transport of positively, neutrally, and negatively buoyant biodegradable MPs from rivers. The results show that positively buoyant MPs have significant seasonal variations and are mainly distributed in the surface layer. Neutrally buoyant MPs are distributed in all water depths, with a high (low) concentration in the eastern (western) Seto Inland Sea (SIS), characterized by winter mixing and summer stratification. Negatively buoyant MPs accumulate in the sediments and exhibit lower concentrations in seawater. Positively and neutrally buoyant MPs mainly outflow from the SIS into the Pacific Ocean, whereas negatively buoyant MPs hardly leave

* Correspondence to: Center for Marine Environmental Studies, Ehime University, 2-5 Bunkyo-Cho, Matsuyama 790-8577, Japan.
E-mail address: guo.xinyu.mz@ehime-u.ac.jp (X. Guo).

https://doi.org/10.1016/j.jhazmat.2025.137911
Received 21 December 2024; Received in revised form 26 February 2025; Accepted 9 March 2025
Available online 11 March 2025

the SIS and are primarily deposited and degraded near river mouths. A settling velocity of -10^{-6} to -5×10^{-5} m s^{-1} (downward) greatly affects the concentration of MPs in seawater. However, large upward and downward velocities outside this range do not result in pronounced changes. Compared with traditional MPs, biodegradable MPs are less environmentally persistent by not accumulating in sediments and keeping a low concentration there, which contributes to the reduction of transport flux of MPs to the Pacific Ocean.

1. Introduction

Environmental pollution owing to microplastics (MPs, <5 mm) has become an increasingly serious global problem [1-4]. Owing to variations in their physical properties (e.g., density, size, and shape), MPs settling and rising velocities also exhibit variability [5-7]. Based on such properties, MPs are classified into three categories: positively buoyant, negatively buoyant, and neutrally buoyant [8]. MPs can also be categorized into biodegradable and non-biodegradable types based on their degradation properties [9]. The fates and trajectories of these distinct types of MPs vary because of physical, chemical, and biological processes in marine environments [10,11].

The settling velocities of MPs in water are strongly influenced by their density and diameter [12], typically increasing proportionally with particle diameters [5,7,12] and density [5]. Based on terminal velocity experiments of oceanic samples and theoretical formulas, the vertical velocities of positively and negatively buoyant MPs range between 10^{-2} (upward) and -1.27×10^{-1} m s^{-1} (downward) [13,14,6,15,16,7].

Furthermore, the transport of MPs in the ocean is controlled by physical processes such as vertical mixing, horizontal transport, deposition, and resuspension [10,11]. These variable external and internal influences cause MPs to exhibit distinct transport dynamics and distribution patterns across various marine environments. Model predictions reveal that MPs in seawater can either float and sink to the sea bottom, or oscillate vertically over time [15]. Globally, positively buoyant MPs are primarily found in surface garbage patches, whereas negatively buoyant MPs are located in the deepest seafloors [8].

In East Asia, the main deposition areas of MPs are the Japan Sea and the Yellow Sea [8]. Transport processes vary with the seas owing to their different regional circulation patterns. For example, the vertical velocity in the China Seas prevents positively buoyant MPs from being transported out to the northwest Pacific Ocean, and the movement distances of negatively buoyant MPs are two orders of magnitude smaller than those of positively buoyant MPs [17]. MPs and mesoplastics are selectively transported by a combination of Stokes drift and terminal velocity in the Seto Inland Sea (SIS) and coastal waters in the Japan Sea [18,19].

Plastics account for approximately 11 % (275 million MT) of municipal solid waste and are emitted from land into the ocean via rivers and wastewater outflows [20-22,4]. Nihei et al. [23] analyzed the numerical and mass concentrations of MPs collected at 185 sites on the surfaces of 147 Japanese rivers and reported that these concentrations showed significant positive correlations with both population density and urban ratio. Notably, the SIS region, one of the most industrialized areas in Japan, has a coastal watershed population that accounts for 24 % of the total population in Japan. MPs have been found in almost all regions of the SIS in seawater, with high abundances in Beppu Bay and Osaka Bay [14,24,18,25]. MPs have also been detected in the sediments of Beppu Bay, with the first fragment found from a 1958.8–1961.0 CE sediment layer [14].

MPs are difficult to degrade quickly and thus remain in the marine environment for long periods [26]. For example, plastics such as polyethylene (PE) carrier bags do not exhibit visible signs of biodegradation in sediments even after 98 d [27]. The weight loss of multilayer plastic materials in sediments is approximately 0.9 % after 1 year [28]. The maximum weight losses of low- and high-density PE and polypropylene (PP) after 6 months in seawater are 0.5–2.5 % [29].

To address these marine environmental pressures, new biodegradable plastics are being developed [30,31]. Degradation in marine environments can induce obvious weight loss in biodegradable materials [28,32,33], with MPs made from different materials degrading at different rates. For example, under seawater (sediment) conditions, the mass loss of polylactic acid was as high as 24.6 % (75.3 %) after 1 year [28]. Polyhydroxyalkanoate particles in marine sediments experienced a 51 % mass loss after 424 d [9].

As the production capacity of such degradable plastics gradually increases, their environmental impact becomes a concern [34,30,31]. Furthermore, the generation of ocean plastic debris and its observed abundance in oceans is imbalanced [35,36,20,37]. This makes the determination of the distribution and transport processes of MPs difficult through observations alone, thereby necessitating further exploration and clarification [37,38].

Thus, this study uses a hydrodynamic model to investigate the fate and mass budget of riverine (land-derived) MPs in the SIS. By treating MPs as passive tracers with a vertical velocity and simulating three types of biodegradable MPs, we intend to determine when and where MPs accumulate in the water column and sediments. The results of this study provide fundamental information to minimize the harm of MPs to humans and the marine ecosystem.

2. Model configuration

2.1. Study area

The SIS is the largest semi-enclosed coastal sea in Japan. Its geographical extent and bathymetric distribution are shown in Fig. 1. The average depth is approximately 38 m, with the deepest area located near the Hayasui Strait, which connects Iyo-Nada ("nada" refers to broad basins separated by islands and narrow straits) to the Bungo Channel. Except for Iyo-Nada and Beppu Bay, the coastal areas of SIS are relatively shallow, with depths of < 60 m. The river systems around the SIS consist of 21 first-order rivers and many second-order rivers. The intrusion of shelf water into the SIS through the Bungo and Kii Channels is influenced by perturbations of the Kuroshio, one of the strong western boundary currents in the Pacific Ocean [39-41]. Significant seasonal variation occurs in the circulation of this region, exhibiting different summer and winter patterns under the control of tidal mixing, surface heating, riverine freshwater, and wind forces [42].

SIS is one of the most heavily impacted marine environments in Japan due to its proximity to highly industrialized and urbanized regions, leading to considerable anthropogenic input, including MPs pollution [23]. The concentration of MPs in the SIS is 1.2 times higher than the world average value [43] and MPs pollution is at medium to high levels [44]. This region exhibits geographical difference, with dense urban development in the east and predominantly rural and agricultural lands in the west. Its semi-enclosed nature and relatively slow water exchange with open ocean make it particularly susceptible to the accumulation and retention of pollutants [45,46]. In addition, the SIS is an ecologically important area characterized by abundant fisheries resources and marine biodiversity [47]. It is crucial to assess the potential threats posed by MPs pollution.

2.2. Hydrodynamic module

Based on the Princeton Ocean Model [48], a hydrodynamic model for the SIS has been established to simulate the seasonal variation of water circulation [42] and the dispersion of dissolved pollution matter

from rivers in the SIS [49]. This model has been validated in previous studies through extensive comparisons of simulated results with observational data, including temperature, salinity, and current fields in the SIS [42,49].

The model has a horizontal resolution of 1/120° in the meridional direction, 1/80° in the zonal direction, and 21 sigma layers in the vertical direction. The model used climatology daily data to drive the hydrodynamic module, including sea surface temperature, wind stress, shortwave and longwave radiations, sensible and latent heat fluxes. The open boundary conditions, including the tidal current and subtidal current, water temperature, salinity, and surface elevation, were derived from a robust diagnostic model by Guo et al. [50]. The model domain included 21 first-order rivers and five second-order rivers (Fig. 1). Daily river discharges from 1993 to 2016 were obtained from the Ministry of Land, Infrastructure, and Transport, and their climatology daily data were used in the model. Further details of this model can be found in Zhu et al. [49] and Chang et al. [42].

2.3. MPs transport module

2.3.1. Processes of the riverine MPs in the SIS

Rivers and streams are widely recognized as the primary sources of MPs in coastal oceans [21]. In this study, we considered the riverine MPs input into the SIS as the only MPs source. As initial conditions, no MPs were transported into the seawater and sediments.

The physical and biogeochemical processes controlling the behavior of MPs in the SIS are advection and diffusion, deposition, resuspension, and degradation processes (Fig. 2). Correspondingly, the fates of riverine MPs into the SIS are outflow to the open ocean, sinking into the sediment, degradation in seawater and sediment, and retention in the SIS (Fig. 2).

The mass budget of MPs in Fig. 2 can be summarized by Eqs. (1)–(3):

$$Mass_{river\ input} = Mass_{seawater} + Mass_{sinking} + Mass_{outflow} + Mass_{pelagic\ degradation} \quad (1)$$

$$Mass_{sinking} = Mass_{sediment} + Mass_{benthic\ degradation} \quad (2)$$

$$Mass_{outflow} = Mass_{Bungo\ Channel} + Mass_{Kii\ Channel} \quad (3)$$

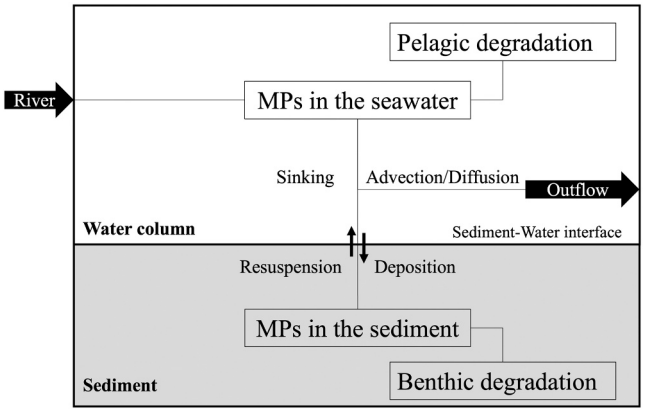

Fig. 2. Conceptual scheme of the microplastics (MPs) transport module.

where the total mass of river input ($Mass_{river\ input}$) is balanced by those remaining in the seawater ($Mass_{seawater}$), sinking into the sediment ($Mass_{sinking}$), outflowing to the open ocean ($Mass_{outflow}$), and degrading in seawater ($Mass_{pelagic\ degradation}$). The mass of sinking into the sediment is balanced by those remaining in the sediment ($Mass_{sediment}$) and degrading in sediment ($Mass_{benthic\ degradation}$). The mass of outflow to the open ocean has two exits, the Bungo ($Mass_{Bungo\ Channel}$) and Kii ($Mass_{Kii\ Channel}$) Channels.

2.3.2. Governing transport equation

Generally, Eulerian and Lagrangian approaches are used to solve particle transport problems. The Lagrangian approach focuses more on the movement of individual particles, whereas the Eulerian framework characterizes particles based on their mass or volumetric concentrations [8]. As this study focuses on the distribution pattern of concentration of MPs instead of the behavior of individual particles, the Eulerian approach was more appropriate for calculating the budget and distribution of MPs in the SIS.

The three-dimensional advection–diffusion equation for the transport of MPs in seawater is given in Eq. (4), and the change of mass in sediments in Eq. (5):

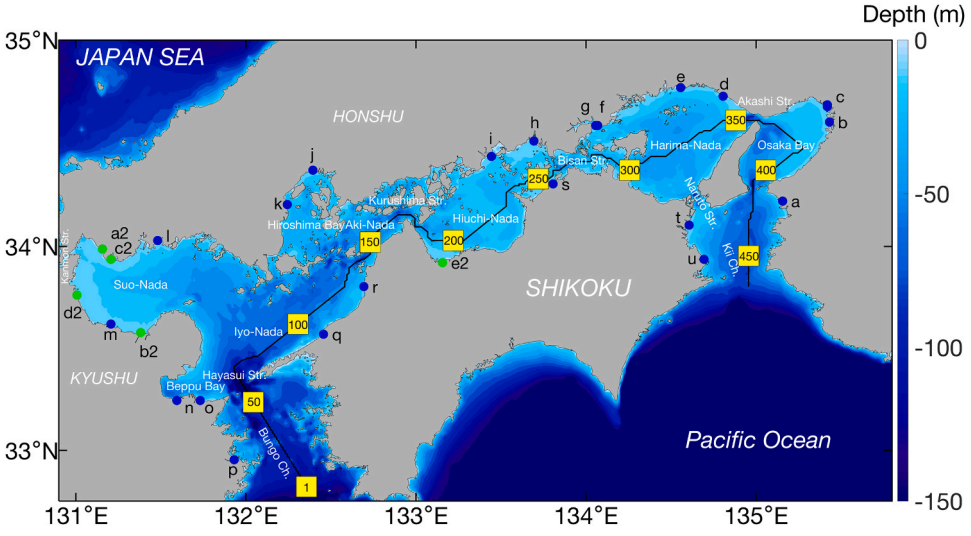

Fig. 1. Bathymetry (m) of the model domain. The blue and green dots along coast denote the positions of first- and second-order rivers, respectively. The black line and solid yellow squares with number from 1 to 450 denote selected section used in Fig. S4–S6.

Table 1
Setting velocity for model calculations (Cases 1–3).

Case	MPs type	Property	Settling velocity	State of motion	Biodegradable
1	Positively buoyant	Low density	10^{-2} m s^{-1}	Rising	Yes
2	Neutrally buoyant	Small MPs and nanoplastics	0 m s^{-1}	Stationary	Yes
3	Negatively buoyant	High density	-10^{-2} m s^{-1}	Sinking	Yes

$$\frac{\partial C}{\partial t}+\frac{\partial UC}{\partial x}+\frac{\partial VC}{\partial y}+\frac{\partial (W+W_s)C}{\partial z}=\frac{\partial}{\partial x}\left(A_H\frac{\partial C}{\partial x}\right)+\frac{\partial}{\partial y}\left(A_H\frac{\partial C}{\partial y}\right)+\frac{\partial}{\partial z}\left(K_H\frac{\partial C}{\partial z}\right)+S \tag{4}$$

$$\frac{\partial M}{\partial t}=-E_b+S_{sed} \tag{5}$$

where W_s is the MPs settling velocity, A_H is the horizontal diffusion coefficient, K_H is the vertical diffusion coefficient, S and S_{sed} are the terms for sources or sinks in the water column and sediment, M is the mass for unit area, and E_b is the net sediment flux. Depending on their physical properties (e.g., density, size, and shape), MPs exhibit different behaviors in the water column. Thus, we considered three types of MPs with different settling velocities (Table 1).

2.3.3. Biodegradation process

We considered the degradation process as the only source–sink term for the MPs in seawater and sediment, with the equations given as follows.

$$S=-\gamma_w C \tag{6}$$

$$S_{sed}=-\gamma_{sed} M \tag{7}$$

where γ_w is the pelagic degradation coefficient and γ_{sed} is the benthic degradation coefficient. Based on the experimental data provided by Kureha Corporation (Method S1), an exponential function fitting was applied to determine these coefficients (Fig. S1). Because the degradation rates of plastics vary widely, four groups of degradation experiments were conducted to characterize the impact of the degradation process (Table 2). In the first group (No. 1 in Table 2), the degradation rates of biodegradable MPs in seawater and sediment were given by fitting the measurements in the laboratory. This group of parameters was applied to Cases 1–3. In the fourth group (No.4 in Table 2), observations of non-biodegradable materials [29] were used (Fig. S2) to fit the degradation coefficients of non-biodegradable MPs (traditional MPs) under the assumption that the degradation rates in seawater and sediment were the same. The second and third groups used values that were intermediate between those of the first and fourth degradation rates (Table 2). The last three groups of parameters were applied to a sensitivity analysis.

2.3.4. Boundary conditions

The surface and bottom boundary conditions for the MPs in the seawater are as follows:

Table 2
Groups of different degradation parameters.

No.	Data source	γ_w(d^{-1})	γ_{sed}(d^{-1})
1	γ_{w1}, γ_{sed1}	7.352×10^{-4}	4.818×10^{-3}
2	$\gamma_{w2}=(\gamma_{w1}+\gamma_{w4})/2$, $\gamma_{sed2}=(\gamma_{sed1}+\gamma_{sed4})/2$	3.985×10^{-4}	2.440×10^{-3}
3	$\gamma_{w3}=\gamma_{sed3}=\gamma_{w2}$	3.985×10^{-4}	3.985×10^{-4}
4	γ_{w4} [29], $\gamma_{sed4}=\gamma_{w4}$	6.187×10^{-5}	6.187×10^{-5}

$$K_H\frac{\partial C}{\partial z}=0,\quad z=\eta \tag{8}$$

$$K_H\frac{\partial C}{\partial z}=E_b,\quad z=-H \tag{9}$$

where η is the surface elevation and H is the water depth. According to Ariathurai and Krone [51], E_b is employed to estimate the net sediment flux, which involves deposition (D_e) and resuspension (R_e) processes, as shown in Eq. (10):

$$E_b=\begin{cases} D_e=C_b w_s\left(\dfrac{|\tau_b|}{\tau_c}-1\right), & \text{if } |\tau_b|<\tau_c \\ R_e=E_0\left(\dfrac{|\tau_b|}{\tau_c}-1\right), & \text{if } |\tau_b|>\tau_c \end{cases} \tag{10}$$

where C_b is the concentration of MPs in the bottom layer, τ_b is the bottom stress, τ_c is the critical stress for resuspension and deposition, and E_0 is the erosion coefficient. The erosion coefficient E_0 is usually assumed to be a constant [52-55]; in this study, its value was set to 10^{-6} kg m^{-2} s^{-1}. Furthermore, R_e is limited by the amount of MPs inside the sediments; that is, if no MPs are left in the sediment, R_e is specified as zero.

Notably, the MPs erosion mechanism remains unclear [56]. Compared with typical sediments such as mud and sand, the MPs content in sediments is not dominant. Therefore, we assumed that MPs would not affect the resuspension process of sediments but would appear during the resuspension process. Considering the sediment distribution in the SIS [57], we set τ_c as 0.14 N m^{-2}, which was previously used by Ballent et al. [13].

2.3.5. River input

We directly observed the concentration of MPs in ten rivers (Table 3) to obtain the flux of riverine MPs into the sea. To quantify the concentration of MPs in the other rivers we did not observe, we grouped the ten rivers into three categories according to the population living in their watersheds. The average concentrations in the three groups were used as a reference to estimate the concentration of MPs in the other rivers from the related population. After determining the concentration of MPs, the flux of MPs in each river was given by multiplying the daily river discharge and concentration of MPs, which was treated as a constant throughout the calculation.

2.4. Model validation

Because the MPs in the SIS were mainly sampled in the surface layer [14,24,18], we used the calculation results with positively buoyant non-biodegradable MPs by applying the settling velocity in Case 1 and the degradation parameters in No. 4 (Table 2) to validate the model. For

Table 3
Concentrations of the riverine MPs Nihei et al. [23].

No.	River	Population (ten thousand)	Concentration (mg m^{-3})
a	Kino	67	0.024
b	Yamato	215	0.373
c	Yodo	1100	0.111
g	Asahi	33	0.044
l	Saba	3	0.001
q	Hiji	10	0.001
r	Shigenobu	24.4	0.055
s	Doki	3.9	0.844*
t	Yoshino	61	0.009
u	Naka	4.7	0.057
others	others	≤10	Average = 0.020
		≤100	Average = 0.033
		>100	Average = 0.242

Note: The value with an asterisk (*) was not used to calculate the average.

such a comparison, the mass concentration in the model results must be converted into a unit of piece numbers per unit volume of seawater [58]. We used a 0.3 mm particle size to calculate the mass of each particle [58]. As PE and PP are the main polymer types in the surface layer of the SIS, their mean density (0.9 g cm^{-3}) was used in the conversion [14,18].

The model results of MPs in the seawater have the same order of concentration and similar spatial distribution as the observations (Fig. S3). Specifically, the model results and observations both show a high MPs abundance in the head of Beppu Bay and a decrease of MPs concentration from the bay head to the bay mouth. In the areas close to the coast, the model resolution is too low to resolve nearshore processes and the difference between model results and observations is a little large. MPs < 0.3 mm were unlikely to be captured because of the size of the net used for sampling. In addition, trawl sampling was mainly conducted at the sea surface and could not observe the abundance in the subsurface and bottom layers. We complemented the observations with numerical simulations and analyzed the characteristics of the spatio-temporal variations of the different types of MPs in the model results.

3. Results

3.1. Seasonal variation of positively, neutrally, and negatively buoyant MPs in the seawater and sediment

We examined the spatiotemporal variations of the three types of biodegradable MPs in the SIS using Cases 1–3 (Table 1) with the degradation parameters of No. 1 (Table 2). The model was initialized on the first day of January with zero concentration of MPs at all the grid points. The spatially averaged concentration (C_v) of MPs in the seawater over the entire SIS showed a stable seasonal variation in the third and fourth years. Therefore, the model results of the fourth year were used in the analysis (Fig. 3).

The concentration of positively buoyant MPs in the seawater rapidly increased from April to September and decreased from September to December, showing a peak of 1.65×10^{-3} mg m^{-3} in mid-September (Case 1 in Fig. 3). A slight fluctuation and decrease were observed from January to March.

Compared with positively buoyant MPs, neutrally buoyant MPs in the seawater (Case 2 in Fig. 3) presented a smaller range of seasonal variation and an earlier peak. The concentration of the neutrally buoyant MPs increased from January to July, and then decreased until December, reaching a peak of 1.56×10^{-3} mg m^{-3} in late July. Their concentration was generally higher than that of positively buoyant MPs, except in August, September, and October.

Negatively buoyant MPs showed a lower concentration in the seawater than the other two types of MPs by two orders (Case 3 in Fig. 3). Those from rivers rapidly sunk after leaving the river mouth and were deposited onto the sediments. Their concentration in the seawater increased minimally in June, peaking at approximately 7.9×10^{-6} mg m^{-3}, and subsequently decreased from July to December.

No positively and neutrally buoyant MPs were found in the sediment owing to the lack of a deposition process. The mass of negatively buoyant MPs in the sediment showed a stable lower value from March to April, increased in May, and reached the highest value from late September to early October (Fig. 4). Subsequently, it gradually decreased until the following year.

3.2. Spatial variation of positively buoyant MPs during the four seasons

The vertically averaged concentrations of positively buoyant MPs in the seawater showed different horizontal distributions during the four seasons (Fig. 5). In winter and spring, narrow bands of high concentration were found along the south or southeast coasts of Iyo-Nada, Harima-Nada, Hiuchi-Nada, Bisan Strait, and Osaka Bay. In summer, concentrations were high over a relatively large area and still formed a band along the north or northwest coasts of Beppu Bay, Suo-Nada, Hiroshima Bay, Aki-Nada, Hiuchi-Nada, Bisan Strait, Harima-Nada, and Osaka Bay. The distribution pattern in autumn differed from that in summer, showing high concentrations along the south coast of Suo-Nada, Bisan Strait, and the western area of Harima-Nada. Meanwhile, the concentration in Osaka Bay decreased. Owing to their settling velocities, MPs exhibit different distributions and behaviors in the marine environment [59]. Some MPs float at the surface, and others are suspended and oscillate in the seawater or sink to the seafloor [60,14,15,61]. Because of their upward velocity, positively buoyant MPs (Case 1) rise in the water column until they reach the sea surface and consequently accumulate at the sea surface (Fig. S4 and Fig. S5). The simulated profiles show that positively buoyant MPs are present in the top 0–5 m of the water column. According to the measurements of the depth profile and the one-dimensional column model of positively buoyant MPs, the concentration of MPs decreases exponentially with depth, and MPs with lower upward velocities are more susceptible to wind mixing [16].

The positively buoyant MPs present apparent seasonal variations in the surface layer (Fig. S5). In January and April, a high concentration of MPs was observed in areas shallower than 5 m. In July and October, these high-value areas were deepened, with MPs becoming more strongly vertically mixed in the regions of Aki-Nada to Hiuchi-Nada, the Bisan Strait, the Harima-Nada, the Akashi Strait, and the Kii Channel (Fig. S4). Owing to variations in MPs transport, only the bottom layer in

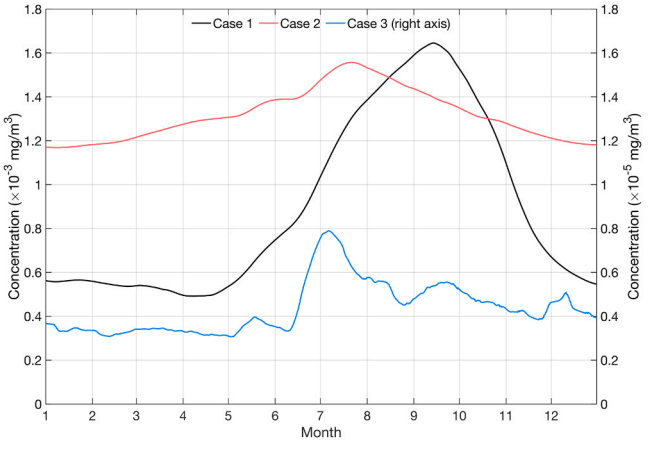

Fig. 3. Time series of the spatially averaged concentration of MPs in the seawater over the entire Seto Inland Sea (SIS) during the fourth computational year in Cases 1–3. A low pass filter (15- days running mean) was applied to the hourly data to remove the tidal variations. The left axis is for Cases 1 and 2. The right axis is for Case 3.

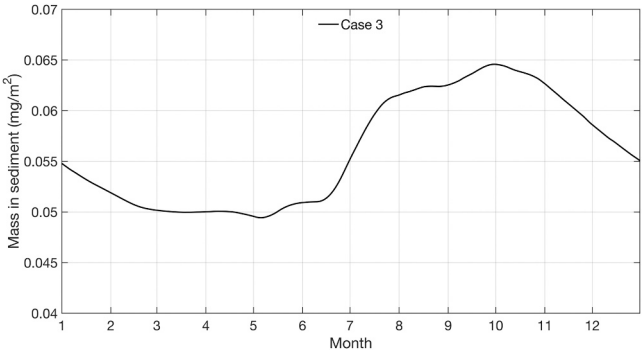

Fig. 4. Time series of the spatially averaged mass of MPs in the sediment over the entire SIS during the fourth computational year in Case 3. A low pass filter (15- days running mean) was applied to the hourly data to remove the tidal variations.

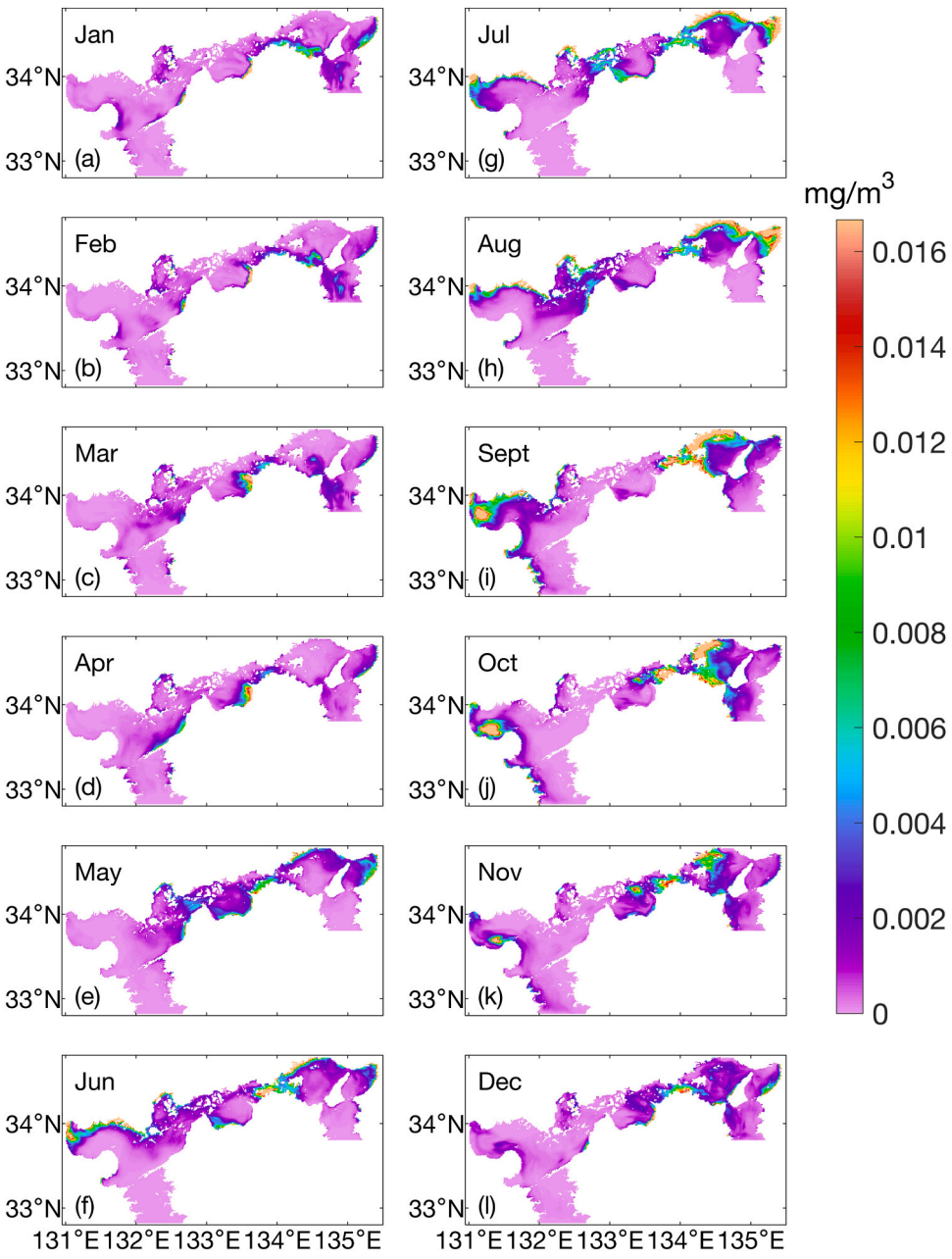

Fig. 5. Monthly mean of the vertically averaged concentration of MPs in the water column in Case 1.

the Bisan Strait remained at a high concentration in October.

The accumulation of positively buoyant MPs on the sea surface formed a band along the south coast in winter and the north coast in summer. This is likely related to the prevailing northwesterly winds in winter and the prevailing southeasterly winds in summer, which induces the convergence of surface water in the areas with high concentrations of positively buoyant MPs. In addition to the winds, the local circulations in Osaka Bay related to the river plume are the cause for the high concentration in the head of Osaka Bay in summer. The geostrophic balance with the density field through thermal wind relationships leads to the formation of a cyclonic circulation in Suo-Nada, Hiuchi-Nada, and Harima-Nada in summer [42], which also promotes the positively buoyant MPs accumulated in the coastal areas. Beginning in the autumn, the nearshore transport of positively buoyant MPs followed a trajectory of the outflow along the western coast from the channels to the open sea (Fig. 5).

3.3. Spatial variation of neutrally buoyant MPs during the four seasons

Zero settling velocity was used to simulate neutrally buoyant MPs (Case 2), which represented small MPs and nanoplastic particles [8]. Neutrally buoyant MPs are more widely distributed from the river than other MPs (Fig. 6). In winter, their overall concentrations were relatively low, with slightly higher concentrations in Hiroshima Bay, Harima-Nada, and Osaka Bay. From spring to summer, concentrations began to increase in the same regions where they had been relatively high. In autumn, the concentrations decreased slightly. In Osaka Bay, these MPs were consistently present at high concentrations throughout the year, owing to the influence of the Yodo River. Overall, high concentrations were observed in the eastern region and low concentrations in the western region of the SIS. Neutrally buoyant MPs neither sink nor rise in the seawater, which means that their particles are distributed at all depths because of eddy diffusion. The vertical distribution is likely controlled by the stratification. The surface and bottom concentrations

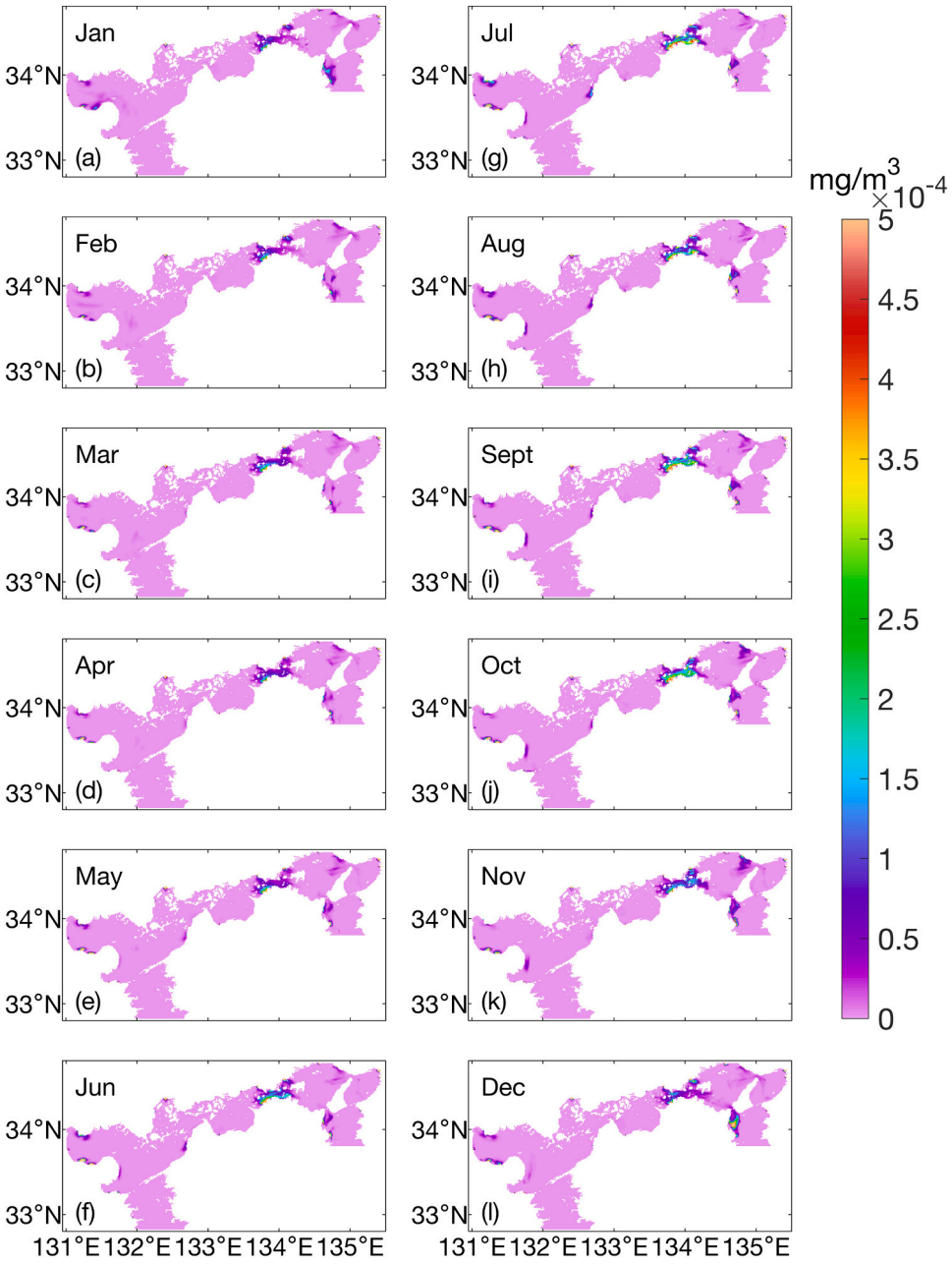

Fig. 6. Monthly mean of the vertically averaged concentration of MPs in the water column in Case 2.

were essentially homogeneous in January but varied in July, which was dependent on stratification in summer and vertical mixing in winter (Figs. S4 and S5).

3.4. Spatial variation of negatively buoyant MPs during the four seasons

Negative buoyancy represents particles that settle in seawater owing to their physical properties. Their concentrations in the seawater were relatively low, except in the areas close to river mouths (Fig. 7). Notably, the Bisan Strait is likely a convergence zone for this type of MPs because of its strong tidal mixing as well as the inflows from the western and eastern SIS [42].

The vertical distribution of negatively buoyant MPs differed from those of the other types of MPs. High concentrations were concentrated near the seafloor (Figs. S5 and S6). The depth of maximum concentration was between 20 and 30 m in the Bisan Strait. For negatively buoyant MPs, downward settling velocity reduces the seasonal difference in surface concentrations but increases that in bottom concentrations.

Corresponding to the concentrations in seawater, negatively buoyant MPs in the sediment were mainly distributed and accumulated near the river mouth (Fig. 8). Their concentrations in the sediments decreased outward with the distance from the estuary. Over the entire SIS, negatively buoyant MPs were deposited in Beppu Bay, Suo-Nada, Hiroshima Bay, Harima-Nada, Osaka Bay, Kii Channel, and along other coastal regions. They were rarely deposited near the straits because of the large bottom shear stress that easily makes them leave the sea bottom.

4. Discussion

4.1. Key factors responsible for seasonal MPs variation

Seasonal variations in the concentration of MPs in seawater are affected by riverine inputs, pelagic degradation, sinking to sediment,

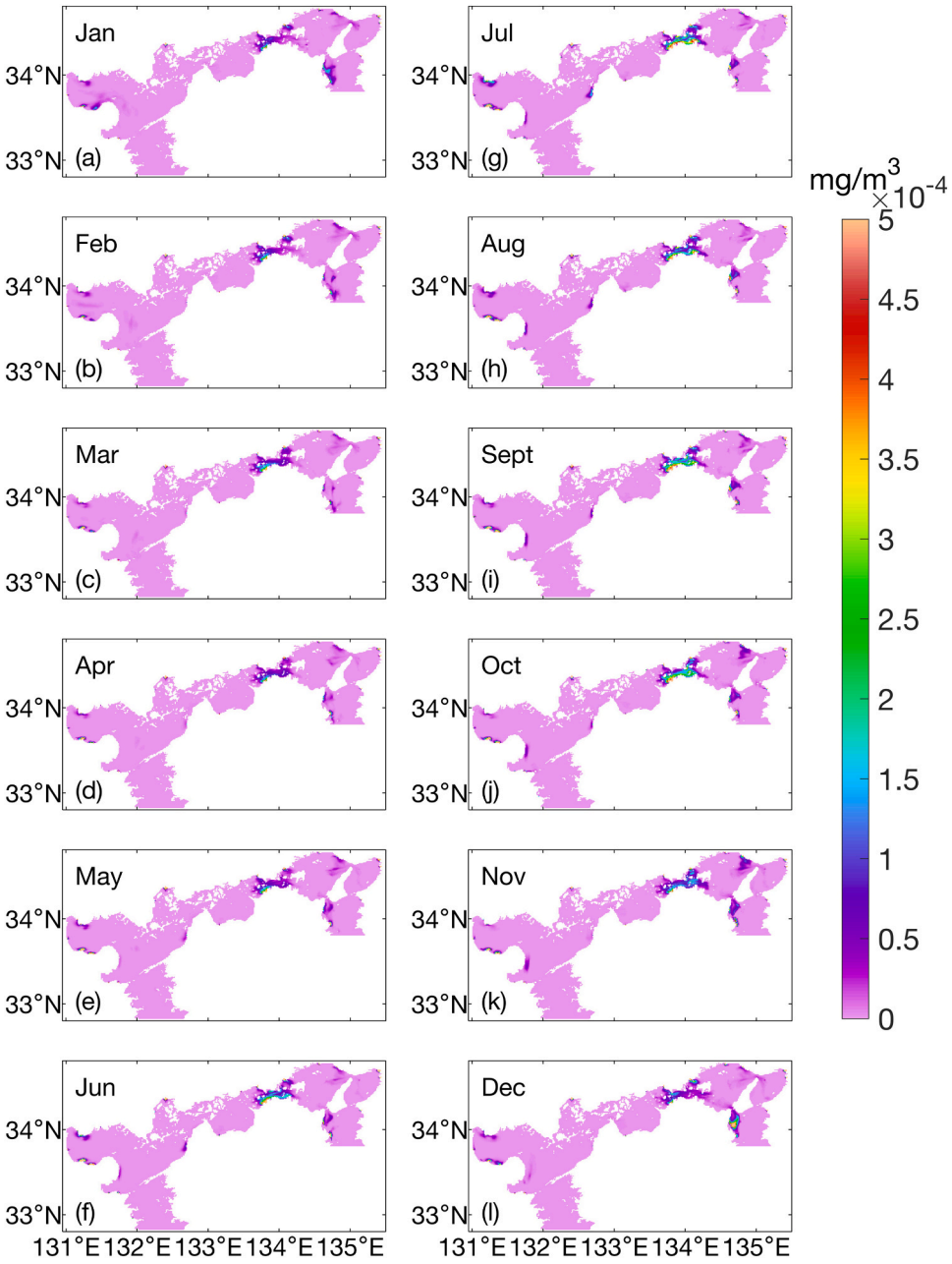

Fig. 7. Monthly mean of the vertically averaged concentration of MPs in the water column in Case 3.

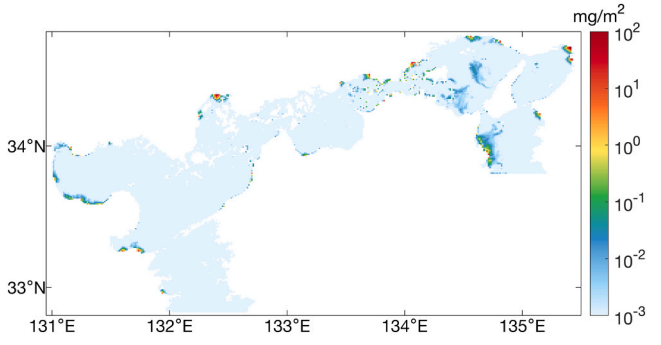

Fig. 8. Mass density of MPs in the sediment in Case 3 on the last day of the fourth year.

and outflow (Fig. 9). Furthermore, the concentration of MPs in sediment is determined by processes including deposition, resuspension, and benthic degradation (Fig. 9).

The SIS exhibits a distinct seasonal rainfall pattern, with increased precipitation during the summer months. This leads to higher river discharge in the summer. Driven by rainfall, all three types of MPs concentrations in seawater demonstrated a marked increase in June (Fig. 3).

In addition to this shared trend, the concentrations of the three types of MPs in seawater showed notable seasonal variations, even when subjected to identical hydrodynamic conditions.

The disparity in the concentrations of positively and neutrally buoyant MPs can primarily be attributed to fluctuations in the outflow flux, as illustrated in Fig. 9a and b. Conversely, the seasonal variations observed in negatively buoyant MPs are predominantly influenced by the sinking flux, as depicted Fig. 9c. For positively buoyant MPs, a lagged correlation was observed between the outflow and river input,

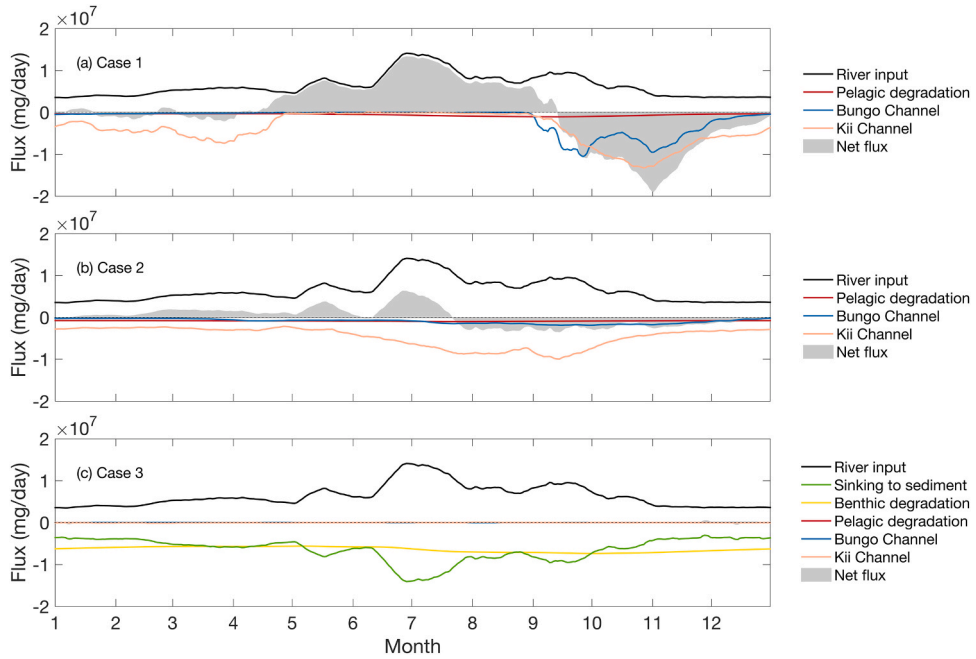

Fig. 9. Time series of the mass flux for river input, pelagic degradation, Bungo Channel outflow, Kii Channel outflow, sinking into the sediments, benthic degradation, and net flux into seawater within the SIS. The dashed line represents zero.

exhibiting a significant positive correlation coefficient of R = 0.75 ($p < 0.01$), with a lag time of 116 d (Fig. S7). The seasonal variation of positively buoyant MPs is significantly influenced by surface currents. During the summer, the seawater in several Nadas becomes highly stratified, leading to the formation of several bottom cold domes and resulting in stable cyclonic eddies [42]. Under this circulation pattern, positively buoyant MPs are primarily distributed near the coast and in the Bisan Strait. Furthermore, the influence of southerly winds generates a northward surface current, which impedes the transport of these MPs to the open ocean in summer [42,49]. Consequently, positively buoyant MPs barely left the SIS, and the fluxes of both channels were almost negligible during this time. The timescales associated with the southerly winds are approximately aligned with the lag times observed in the correlation between outflow and river input.

As autumn approaches and surface cooling starts, the cold eddy structures gradually disperse and the cyclonic eddies during the summer start to weaken [42]. On the other hand, as a part of basin-scale estuarine circulation, the surface outflows toward the Kii Channel and Bungo Channel exists in summer and continues in autumn [42]. Consequently, the MPs initially concentrated along the coast and in the Bisan Strait gradually disperse and are transported through these two channels into the Pacific Ocean. Their peak outflow occurs at the end of October. The intensified southward surface current patterns are attributed to stronger northward wind forces during the fall and winter, which increase the flow velocity by approximately 3.5 cm s^{-1} [49]. Due to the surface circulation, a large amount of positively buoyant MPs outflow from the Kii Channel from the fall season through the subsequent spring, with flux values considerably exceeding those of neutrally buoyant MPs in both channels.

In contrast, the seasonal variation observed in Case 2 was not pronounced. Neutrally buoyant MPs do not accumulate within the surface layer. Therefore, the effect of wind-induced surface circulation was not significant. A lagged correlation was observed between the outflow and river input of neutrally buoyant MPs, demonstrating a significant positive correlation of R = 0.79 ($p < 0.01$), with a lag time of 29 d (Fig. S8). This lag time is approximately equivalent to the duration required for the contaminant to be transported from the river mouth to the open ocean [49]. However, the seasonal cycle of air-sea heat flux influences the seasonal variation of pollutant concentrations by affecting horizontal ocean currents and vertical stratification [49]. In autumn and winter, sea surface cooling enhances vertical mixing of water column and leads to a uniform distribution of neutrally buoyant MPs. In spring and summer, surface heating induces and keeps the stratification of water column, which causes neutrally buoyant MPs to stay in the surface layer and therefore reduces their transport to deep water.

Negatively buoyant MPs (Case 3) rapidly sink to sediment once input from rivers, resulting in the absence of any lag time associated with the outflow. These MPs showed a significant positive correlation between their concentration in seawater and the flux of riverine input (R = 0.83, $p < 0.01$), as well as a significant negative correlation with the sinking flux (R = –0.84, $p < 0.01$).

The degradation flux of MPs was influenced by their concentration in both seawater and sediment. This variation was consistent with the seasonal fluctuations observed in their concentrations within these environments (Fig. 3, Fig. 4, and Fig. 9).

4.2. *Particle velocity sensitivity analysis*

As discussed in Section 3, the settling velocity plays a critical role in governing the transport of MPs within the marine environment and affects their ultimate deposition sites and concentration levels. To effectively evaluate the environmental dynamics and potential repercussions of MPs, sensitivity analyses concerning settling velocity must therefore be performed. In this study, a range of 16 distinct settling velocities was established, spanning from 10^{-1} to -10^{-1} m s^{-1}, with increments of either 5 or 10 times.

We scaled the vertical concentrations of MPs in the seawater over the entire SIS using min-max normalization and present their distribution patterns across all settling velocity range in Fig. S9. Within this velocity range, the concentration varies vertically, with a substantial portion extending from the surface to the bottom. As the upward velocity decreases, the concentration of MPs declines in the surface layer but increases in the subsurface layer. When the downward velocity is large, a high percentage of MPs sink to the bottom. For MPs with settling velocity close to zero, they are more susceptible to vertical mixing and turbulence and thus distribute in the middle layer without being able to

rise rapidly to the surface layer or sink to the bottom layer.

Fig. 10 shows the normalized values of the variables derived from Eqs. 1, 2, and 3. In the case of positively buoyant MPs, the quantity remaining in the seawater showed no clear difference despite the dramatic variation in settling velocity from 10^{-1} to 10^{-5} m s^{-1} (Fig. 10). As the upward velocity decreased from 10^{-1} to 10^{-5} m s^{-1}, the Kii Channel had a corresponding increase in the outflow. Conversely, both the total outflow and the outflow from the Bungo Channel exhibited a continuous decline as the settling velocity transitioned from 10^{-1} to -10^{-1} m s^{-1} (Fig. 10).

The amount of neutrally buoyant MPs remaining in the seawater peaked due to a reduced outflow when compared with positively buoyant MPs, and demonstrated an absence of sinking into the sediment when compared with negatively buoyant MPs (Fig. 10). In the case of negatively buoyant MPs, an increase in the downward settling velocity from -10^{-6} to -5×10^{-5} m s^{-1} resulted in a dramatic reduction in the amount of remaining in the seawater as they rapidly sunk into the sediment (Fig. 10). As the amount remaining in the seawater diminished, a corresponding dramatic decrease in the total outflow was observed. The variation in outflow between the three types of MPs is caused by differences in their distribution within the channels (Fig. S10 and Fig. S11).

The velocity range of -10^{-6} to -5×10^{-5} m s^{-1} was identified as the most sensitive, with the settling velocity increasing by a factor of 50, which resulted in an increase in the proportion of MPs sinking to the sediment from 8 % to 92 %. Consequently, the amount of Kii Channel outflow (total outflow) decreased from 65 % (73 %) to 5 % (6 %). Once the downward settling velocity exceeded -5×10^{-5} m s^{-1}, the amount of MPs remaining in seawater, in the total outflow, and sinking into the sediment exhibited minimal variations. Even with a substantial increase in the settling velocity by a factor of 2000 (from -5×10^{-5} to -10^{-1} m s^{-1}), the changes in the proportions of MPs sinking to the sediment and total outflow were only 7 % and 6 %, respectively.

Negatively buoyant MPs with lower downward settling velocities allow for transport to more remote areas, resulting in deposition in locations distant from the river mouth (Fig. S12). Conversely, negatively buoyant MPs with high downward settling velocities hardly leave the estuary as deposition occurs rapidly following their input from the river (Fig. S12). This phenomenon contributes to a dramatic reduction in outflow from the Kii Channel. Within the SIS, the Yodo River represents the most substantial riverine input. Consequently, this river serves as a case study to elucidate the relationship between increase in the amount of sinking to the sediment and decrease in the amount of outflow from the Kii Channel. The age of Yodo River water indicates that substances input from this river require approximately 60 d to leave the estuarine area, around 120 d for them to be transported to the central region of Osaka Bay, and approximately 180 d to outflow from the SIS via the Kii Channel [62]. At a downward settling velocity of approximately -5×10^{-5} m s^{-1}, particles sink at a rate of about 4.3 m d^{-1} vertically, which corresponds closely to the average depth near the estuary. This suggests that when the downward settling velocity approaches or exceeds this threshold, negatively buoyant MPs will sink to the sediment near the estuary in < 1 d, a duration dramatically shorter than the 60 d required for them to leave the estuary.

The average depths in the estuary, Osaka Bay, and Kii Channel are 7.6, 29.3, and 43.5 m, respectively. Based on the average depths across these regions, if only particle settling (excluding vertical mixing) is considered, the settling velocity must remain below -1.5×10^{-6} m s^{-1} for the particles to leave the estuary and reach the Kii Channel. In summary, the interplay of horizontal and vertical time scales is critical in determining whether negatively buoyant MPs can leave the estuary and reach the Kii Channel.

4.3. Degradation parameter sensitivity analysis

At present, a thorough evaluation of the biodegradation of MPs in marine environment has yet to be conducted [63]. Generally, the degradation process is influenced by both intrinsic polymer factors and external environmental factors [63]. Thus, the degradation rate parameter exhibits considerable uncertainty. By performing sensitivity analyses on the degradation rate, we can investigate its variations in oceanic conditions under diverse scenarios.

The degradation processes of MPs within the SIS indicate a significantly higher level of MPs degradation in sediments than in seawater (Fig. 11). The extent of MPs degradation in both environments is correlated with their concentration in each respective medium and their degradation parameters. Larger degradation parameters correspond to lower concentrations, both in seawater and in sediments. The largest difference in concentration in seawater occurs between biodegradable MPs (No. 1) and non-biodegradable MPs (No. 4), with a value of 0.0002 mg m^{-3} (Fig. S13). For positively buoyant and neutrally buoyant MPs (Fig. 10 and Fig. S13), the concentration of biodegradable MPs (No. 1) in seawater is about 12 % lower than that of non-biodegradable MPs (No. 4).

Similarly, in sediments, the largest difference in mass density is also between No.1 and No.4, with a value of 0.32 mg m^{-2} (Fig. S13). The residual content of biodegradable MPs (No.1) is evidently lower than that of non-biodegradable MPs (No.4) under the same settling velocity

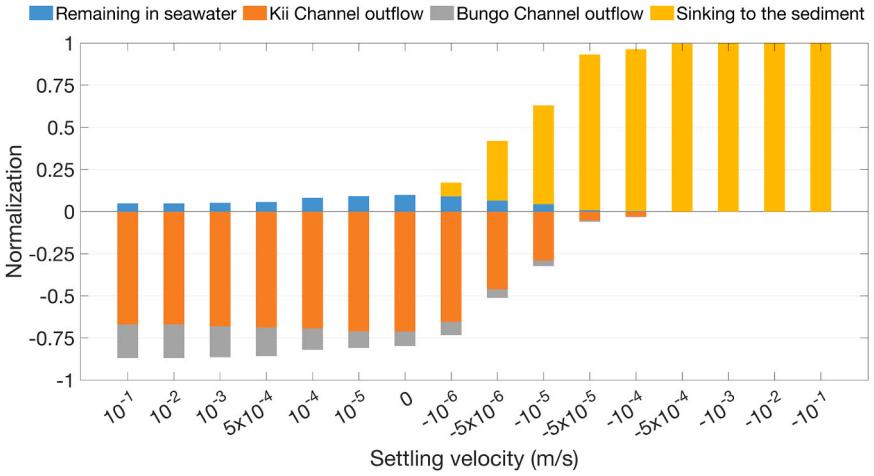

Fig. 10. Relationship between settling velocity and the normalized masses of MPs, including that remaining in seawater, in the Kii Channel outflow, in the Bungo Channel outflow, and sinking into the sediment. A positive value indicates the proportion of riverine MPs retained within the SIS, and a negative value represents the proportion of riverine MPs that either outflow or degrade.

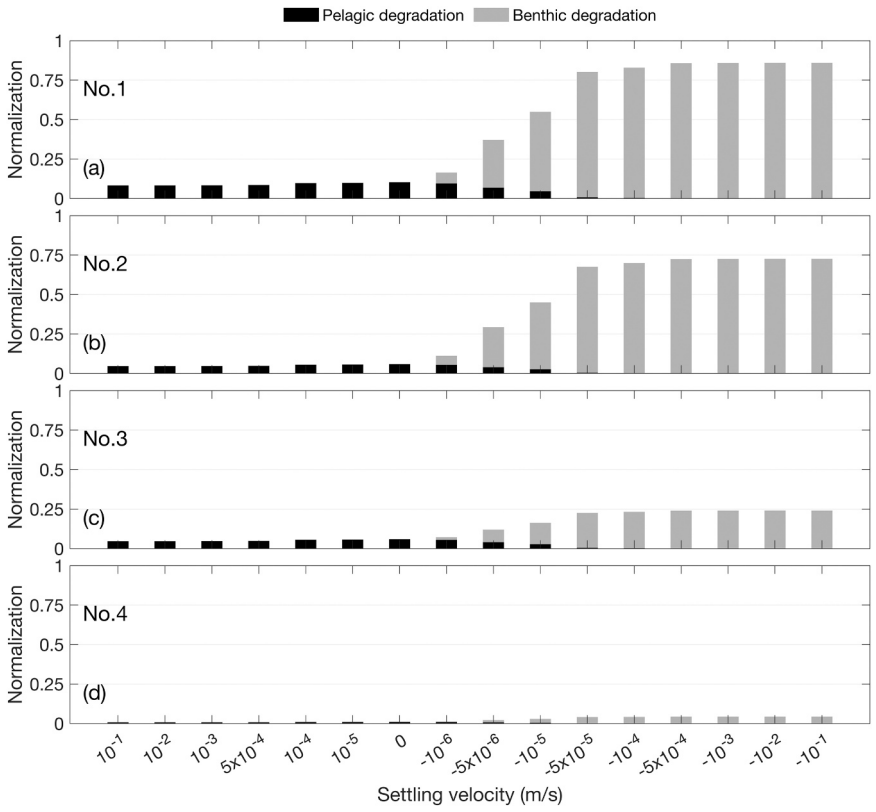

Fig. 11. Relationships between degradation parameters, settling velocity, and the normalized masses of MPs, including pelagic degradation and benthic degradation. (a) to (d) show the results under the different experimental conditions described in Table 2.

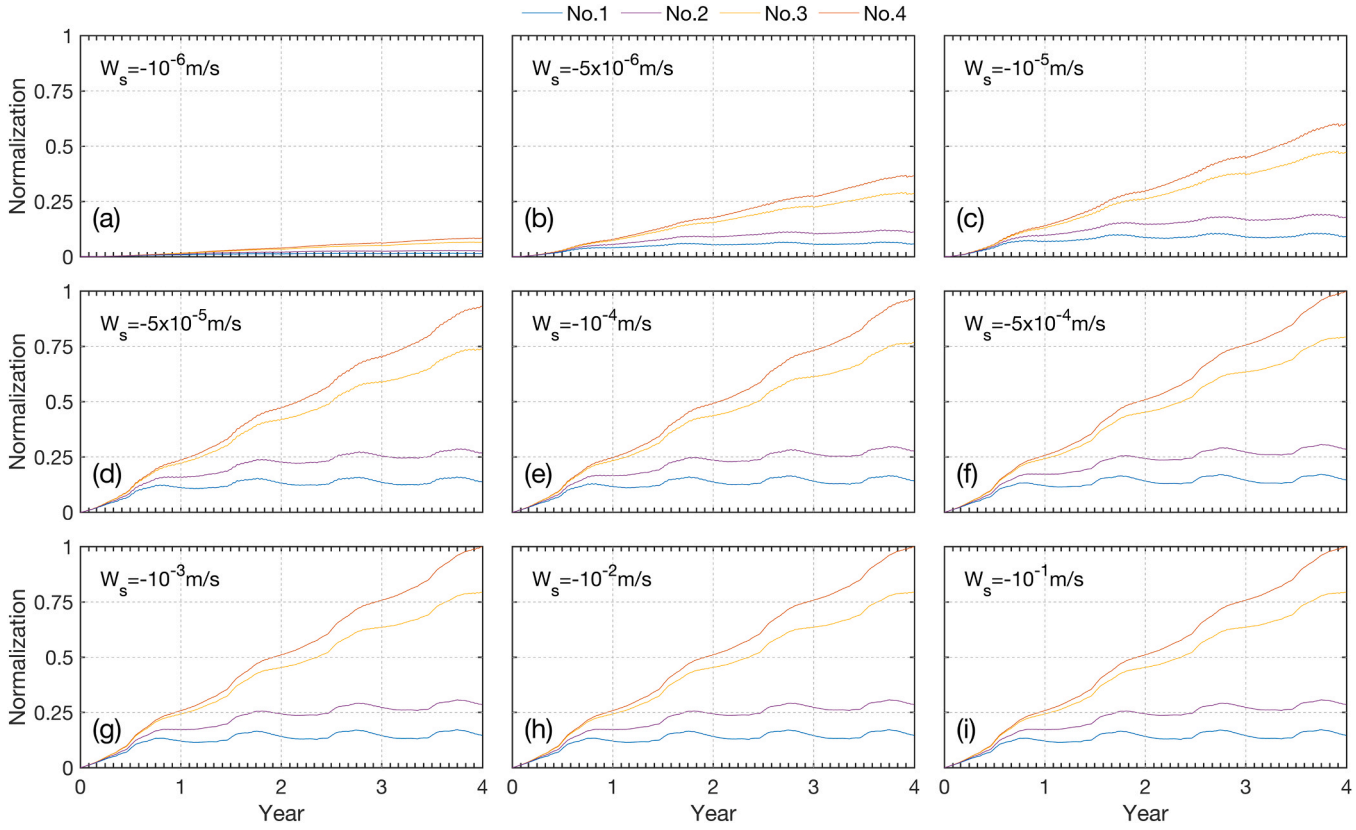

Fig. 12. Time series of the normalized 15-d running mean concentration in sediments over the entire SIS.

(Fig. 12), with the maximum difference between them reaching approximately seven times (Fig. 12). The relative change in the mass of benthic degradation (degradation in the sediment) for biodegradable MPs (No. 1) compared to non-biodegradable MPs (No. 4) exceeds 2000 % (Fig. 11). The simulation analyses concerning non-biodegradable MPs (No.4) revealed a continuous increase in the quantity of negatively buoyant MPs within the sediment (Fig. 12). Owing to their inherent resistance to degradation, these non-biodegradable MPs tended to accumulate persistently on the seafloor once they enter the sediment, rather than undergoing degradation. Additionally, as the settling velocity increased, the capacity of negatively buoyant MPs to leave the estuary diminished progressively, thereby decreasing their outflow through the two channels and further facilitating their accumulation on the seafloor.

As previously indicated, accumulation was observed in all cases of non-biodegradable MPs. Nevertheless, the implementation of biodegradable MPs significantly alleviated this problem (Fig. 12). By the fourth year, the results for both Nos. 1 and 2 reached a state of relative stability, in contrast with the conditions in Nos. 3 and 4. This observation implies that a stable concentration of MPs in the sediment can be attained when the degradation rate (γ_{sed}) exceeds 2.44×10^{-3} d^{-1}, whereas rates below 3.985×10^{-4} d^{-1} are inadequate to fulfill this criterion.

Pelagic degradation does not clearly affect the quantity of MPs remaining in seawater within the SIS. Although the proportion of degradation in seawater increases with the degradation rate, this is offset by a corresponding reduction in outflow through the Kii Channel (Fig. 10, Fig. 11, Figs. S14, S15, and S16). This phenomenon is more pronounced for positively buoyant MPs and neutrally buoyant MPs. Moreover, although the degradation process in seawater does not alter the concentration of MPs within the SIS, the implementation of biodegradable MPs has the potential to diminish the outflow of MPs from the SIS to the Pacific Ocean, thereby contributing to a reduction in MPs pollution in the global marine ecosystem.

5. Conclusions

This study used a three-dimensional ocean model to simulate the transport of biodegradable MPs with different buoyancies within the SIS. The temporal variations and spatial distributions of these buoyant MPs in the riverine input were investigated using river concentration observation data. The mass budget and vertical distribution characteristics of the MPs were determined by varying the particle settling velocities, and the differences between biodegradable and non-biodegradable MPs in the SIS were compared.

The majority of the positively buoyant (neutrally buoyant) MPs flowed into the open sea, with the rest remaining or degrading in seawater. Nearly all of the negatively buoyant MPs were deposited near river mouths and gradually degraded. The concentrations of positively and neutrally buoyant MPs in seawater were markedly higher than those of negatively buoyant MPs. Positively buoyant MPs had greater concentrations in coastal regions and straits, particularly within the surface layer and extending to a depth of 5 m. Neutrally buoyant MPs exhibited high concentrations in the eastern regions and lower concentrations in the west, displaying a uniform distribution throughout the water column. Negatively buoyant MPs tended to accumulate near river mouths and in the Bisan Strait, primarily residing in the bottom layer and sediment.

Variations in the settling velocity do not clearly affect the quantity of positively buoyant MPs remaining in seawater within the SIS. Conversely, an increase in settling velocity from -10^{-6} to -5×10^{-5} m s^{-1} is associated with a marked reduction in the quantity of negatively buoyant MPs remaining in seawater. Furthermore, an excessively elevated settling velocity results in the rapid sinking of negatively buoyant MPs, leading to their deposition in sediments in proximity to the estuary.

Due to their inherent resistance to degradation, non-biodegradable MPs persist for a long time in the ocean. When these MPs sink into sediments, they can accumulate continuously without significant degradation. As the settling velocity increases, the ability of particles to leave the estuary decreases, exacerbating their accumulation on the seafloor. These accumulated non-biodegradable MPs may exacerbate a long-term impact on the environment.

With a higher degradation rate in sediments than in seawater, the biodegradable MPs do not accumulate in the sediments and can eventually reach a stable concentration in the sediments. The degradation of MPs in the sediment and seawater also reduces the outward flux of MPs from the SIS into the Pacific Ocean.

These results reveal the fundamental differences in degradation and accumulation behaviors between biodegradable and non-biodegradable MPs. Biodegradable MPs exhibit a significantly higher degradation rate, especially in sediment environments. When identical quantities of MPs are introduced from rivers, the residual content of biodegradable MPs remains considerably lower than that of non-biodegradable MPs under the same conditions. This indicates that the adoption of biodegradable materials has the potential to substantially alleviate MPs pollution both in sedimentary environments in the SIS and in the open ocean.

This study exclusively examined rivers as the primary source of MPs. However, as MPs have been progressively accumulating along coastal regions, the coast could become an additional source of MPs in the future. Currently, this phenomenon cannot be fully assessed due to insufficient data and the limitation of model resolution. The forcing conditions used in our study are climatological ones and do not account for the abrupt and extreme weather conditions. Future studies should aim to explore the source–sink dynamics of MPs in coastal areas and introduce short-term variations in the model forcing conditions, including river flooding and typhoons. Furthermore, based on our findings, MPs removal initiatives should be implemented in estuarine regions during periods of elevated river discharge, such as the rainy season, to effectively mitigate the influx of MPs into marine environments. Attention should also be directed towards addressing the MPs present in sediments, particularly in estuarine and bay areas.

Environmental implication

A large amount of plastic waste has been discharged into the sea via rivers and wastewater outflows, becoming the main component of waste in the ocean. In addition, traditional MPs are difficult to degrade quickly and thus remain in the marine environment for long periods. The variability in the settling and rising velocities of various types of buoyant microplastics with different degradation capacities influences their fates and trajectories in marine environments, significantly impacting their degradation and accumulation. Numerical simulations can be employed to predict the potential impact of innovative degradable materials in alleviating the burden on the marine environment.

CRediT authorship contribution statement

Li Yaxian: Writing – review & editing. **Zhao Xueting:** Writing – review & editing. **Hinata Hirofumi:** Writing – review & editing, Project administration, Funding acquisition. **Kataoka Tomoya:** Writing – review & editing, Resources, Investigation. **Kikuchi Takako:** Writing – review & editing, Resources, Investigation. **Masaki Takashi:** Writing – review & editing, Resources, Investigation. **Guo Xinyu:** Writing – review & editing, Supervision, Funding acquisition. **Bai Yu:** Writing – original draft, Visualization, Software, Methodology, Funding acquisition, Data curation, Conceptualization.

Declaration of Competing Interest

The authors declare that they have no known competing financial interests or personal relationships that could have appeared to influence

the work reported in this paper.

Acknowledgments

This study was supported by the Moonshot Research and Development Program (Grant Number JPNP18016), the New Energy and Industrial Technology Development Organization (NEDO), and the JST SPRING, Japan (Grant Number JPMJSP2162).

Appendix A. Supporting information

Supplementary data associated with this article can be found in the online version at doi:10.1016/j.jhazmat.2025.137911.

Data availability

Data will be made available on request.

References

[1] Braun, T., Ehrlich, L., Henrich, W., Koeppel, S., Lomako, I., Schwabl, P., Liebmann, B., 2021. Detection of microplastic in human placenta and meconium in a clinical setting. Pharmaceutics 13 (7), 921.
[2] da Costa, J.P., Santos, P.S., Duarte, A.C., Rocha-Santos, T., 2016. Nano) plastics in the environment–sources, fates and effects. Sci Total Environ 566 15–26.
[3] Kane, I.A., Clare, M.A., 2019. Dispersion, accumulation, and the ultimate fate of microplastics in deep-marine environments: a review and future directions. Front Earth Sci 7, 80.
[4] Rochman, C.M., 2018. Microplastics research—from sink to source. Science 360 (6384), 28–29.
[5] Elagami, H., Ahmadi, P., Fleckenstein, J.H., Frei, S., Obst, M., Agarwal, S., Gilfedder, B.S., 2022. Measurement of microplastic settling velocities and implications for residence times in thermally stratified lakes. Limnol Oceanogr 67 (4), 934–945.
[6] Khatmullina, L., Isachenko, I., 2017. Settling velocity of microplastic particles of regular shapes. Mar Pollut Bull 114 (2), 871–880.
[7] Kowalski, N., Reichardt, A.M., Waniek, J.J., 2016. Sinking rates of microplastics and potential implications of their alteration by physical, biological, and chemical factors. Mar Pollut Bull 109 (1), 310–319.
[8] Mountford, A., Morales Maqueda, M., 2019. Eulerian modeling of the three-dimensional distribution of seven popular microplastic types in the global ocean. J Geophys Res Oceans 124 (12), 8558–8573.
[9] Pinnell, L.J., Conkle, J.L., Turner, J.W., 2022. Microbial succession during the degradation of bioplastic in coastal marine sediment favors sulfate reducing microorganisms. Front Mar Sci 9, 945822.
[10] Alfaro-Núñez, A., Astorga, D., Cáceres-Farías, L., Bastidas, L., Villegas, C.S., Macay, K., Christensen, J.H., 2021. Microplastic pollution in seawater and marine organisms across the Tropical Eastern Pacific and Galápagos. Sci Rep 11 (1), 1–8.
[11] Van Sebille, E., Aliani, S., Law, K.L., Maximenko, N., Alsina, J.M., Bagaev, A., Bergmann, M., Chapron, B., Chubarenko, I., Cózar, A., 2020. The physical oceanography of the transport of floating marine debris. Environ Res Lett 15 (2), 023003.
[12] Waldschläger, K., Schüttrumpf, H., 2019. Effects of particle properties on the settling and rise velocities of microplastics in freshwater under laboratory conditions. Environ Sci Technol 53 (4), 1958–1966.
[13] Ballent, A., Purser, A., de Jesus Mendes, P., Pando, S., Thomsen, L., 2012. Physical transport properties of marine microplastic pollution. Biogeosciences Discuss 9 (12), 18755–18798.
[14] Hinata, H., Kuwae, M., Tsugeki, N., Masumoto, I., Tani, Y., Hatada, Y., Kawamata, H., Mase, A., Kasamo, K., Sukenaga, K., 2022. A 75-year history of microplastic fragment accumulation rates in a semi-enclosed hypoxic basin. Sci Total Environ, 158751.
[15] Kooi, M., Nes, E.H.V., Scheffer, M., Koelmans, A.A., 2017. Ups and downs in the ocean: effects of biofouling on vertical transport of microplastics. Environ Sci Technol 51 (14), 7963–7971.
[16] Kooi, M., Reisser, J., Slat, B., Ferrari, F.F., Schmid, M.S., Cunsolo, S., Brambini, R., Noble, K., Sirks, L.-A., Linders, T.E., 2016. The effect of particle properties on the depth profile of buoyant plastics in the ocean. Sci Rep 6, 33882.
[17] Liu, R., Wang, T., Li, J., Liu, X., Zhu, Q., 2023. Simulation of seasonal transport of microplastics and influencing factors in the China Seas based on the ROMS model. Water Res, 120493.
[18] Isobe, A., Kubo, K., Tamura, Y., Nakashima, E., Fujii, N., 2014. Selective transport of microplastics and mesoplastics by drifting in coastal waters. Mar Pollut Bull 89 (1-2), 324–330.
[19] Iwasaki, S., Isobe, A., Kako, Si, Uchida, K., Tokai, T., 2017. Fate of microplastics and mesoplastics carried by surface currents and wind waves: a numerical model approach in the Sea of Japan. Mar Pollut Bull 121 (1-2), 85–96.
[20] Jambeck, J.R., Geyer, R., Wilcox, C., Siegler, T.R., Perryman, M., Andrady, A., Narayan, R., Law, K.L., 2015. Plastic waste inputs from land into the ocean. Science 347 (6223), 768–771.
[21] Lebreton, L.C., Van Der Zwet, J., Damsteeg, J.-W., Slat, B., Andrady, A., Reisser, J., 2017. River plastic emissions to the world's oceans. Nat Commun 8 (1), 1–10.
[22] Meijer, L.J., van Emmerik, T., van der Ent, R., Schmidt, C., Lebreton, L., 2021. More than 1000 rivers account for 80% of global riverine plastic emissions into the ocean. Sci Adv 7 (18), eaaz5803.
[23] Nihei, Y., Ota, H., Tanaka, M., Kataoka, T., Kashiwada, J., 2024. Comparison of concentration, shape, and polymer composition between microplastics and mesoplastics in Japanese river waters. Water Res 249, 120979.
[24] Isobe, A., 2016. Percentage of microbeads in pelagic microplastics within Japanese coastal waters. Mar Pollut Bull 110 (1), 432–437.
[25] Zhou, M., Yanai, H., Yap, C.K., Emmanouil, C., Okamura, H., 2023. Anthropogenic microparticles in sea-surface microlayer in Osaka Bay, Japan. J Xenobiotics 13 (4), 685–703.
[26] Andrady, A.L., 2011. Microplastics in the marine environment. Mar Pollut Bull 62 (8), 1596–1605.
[27] Nauendorf, A., Krause, S., Bigalke, N.K., Gorb, E.V., Gorb, S.N., Haeckel, M., Wahl, M., Treude, T., 2016. Microbial colonization and degradation of polyethylene and biodegradable plastic bags in temperate fine-grained organic-rich marine sediments. Mar Pollut Bull 103 (1-2), 168–178.
[28] Beltrán-Sanahuja, A., Casado-Coy, N., Simó-Cabrera, L., Sanz-Lázaro, C., 2020. Monitoring polymer degradation under different conditions in the marine environment. Environ Pollut 259, 113836.
[29] Sudhakar, M., Trishul, A., Doble, M., Kumar, K.S., Jahan, S.S., Inbakandan, D., Viduthalai, R., Umadevi, V., Murthy, P.S., Venkatesan, R., 2007. Biofouling and biodegradation of polyolefins in ocean waters. Polym Degrad Stab 92 (9), 1743–1752.
[30] Rocca-Smith, J.R., Pasquarelli, R., Lagorce-Tachon, A., Rousseau, J., Fontaine, S., Aguié-Béghin, V., Debeaufort, F., Karbowiak, T., 2019. Toward sustainable PLA-based multilayer complexes with improved barrier properties. ACS Sustain Chem Eng 7 (4), 3759–3771.
[31] Xiong, S.-J., Pang, B., Zhou, S.-J., Li, M.-K., Yang, S., Wang, Y.-Y., Shi, Q., Wang, S.-F., Yuan, T.-Q., Sun, R.-C., 2020. Economically competitive biodegradable PBAT/lignin composites: effect of lignin methylation and compatibilizer. ACS Sustain Chem Eng 8 (13), 5338–5346.
[32] Du, H., Xie, Y., Wang, J., 2021. Microplastic degradation methods and corresponding degradation mechanism: research status and future perspectives. J Hazard Mater 418, 126377.
[33] Zhang, K., Hamidian, A.H., Tubić, A., Zhang, Y., Fang, J.K., Wu, C., Lam, P.K., 2021. Understanding plastic degradation and microplastic formation in the environment: a review. Environ Pollut 274, 116554.
[34] Li, X., Meng, L., Zhang, Y., Qin, Z., Meng, L., Li, C., Liu, M., 2022. Research and application of polypropylene carbonate composite materials: a review. Polymers 14 (11), 2159.
[35] Eriksen, M., Lebreton, L.C., Carson, H.S., Thiel, M., Moore, C.J., Borerro, J.C., Galgani, F., Ryan, P.G., Reisser, J., 2014. Plastic pollution in the world's oceans: more than 5 trillion plastic pieces weighing over 250,000 tons afloat at sea. PloS One 9 (12), e111913.
[36] Isobe, A., Iwasaki, S., 2022. The fate of missing ocean plastics: are they just a marine environmental problem? Sci Total Environ 825, 153935.
[37] Thompson, R.C., Olsen, Y., Mitchell, R.P., Davis, A., Rowland, S.J., John, A.W., McGonigle, D., Russell, A.E., 2004. Lost at sea: where is all the plastic? Science 304 (5672), 838-838.
[38] Woodall, L.C., Sanchez-Vidal, A., Canals, M., Paterson, G.L., Coppock, R., Sleight, V., Calafat, A., Rogers, A.D., Narayanaswamy, B.E., Thompson, R.C., 2014. The deep sea is a major sink for microplastic debris. R Soc Open Sci 1 (4), 140317.
[39] Kaneda, A., Takeoka, H., Nagaura, E., Koizumi, Y., 2002. Periodic intrusion of cold water from the Pacific Ocean into the bottom layer of the Bungo Channel in Japan. J Oceanogr 58, 547–556.
[40] Kobayashi, S., Fujiwara, T., 2009. Modeling the long-term variability of shelf water intrusion into the Seto Inland Sea, Japan. J Mar Syst 77 (3), 341–349.
[41] Morimoto, A., Dong, M., Kameda, M., Shibakawa, T., Hirai, M., Takejiri, K., Guo, X., Takeoka, H., 2022. Enhanced cross-shelf exchange between the Pacific ocean and the Bungo Channel, Japan related to a heavy rain event. Front Mar Sci 746.
[42] Chang, P.-H., Guo, X., Takeoka, H., 2009. A numerical study of the seasonal circulation in the Seto Inland Sea, Japan. J Oceanogr 65 (6), 721–736.
[43] Isobe, A., Uchida, K., Tokai, T., Iwasaki, S., 2015. East Asian seas: a hot spot of pelagic microplastics. Mar Pollut Bull 101 (2), 618–623.
[44] Ahm, E.K., Sekine, M., Imai, T., Yamamoto, K., 2020. Microplastics pollution in the Seto Inland Sea and Sea of Japan surrounded Yamaguchi Prefecture Areas, Japan: abundance, characterization and distribution, and potential occurrences. J Water Environ Technol 18 (3), 175–194.
[45] Takeoka, H., 1984. Exchange and transport time scales in the Seto Inland Sea. Cont Shelf Res 3 (4), 327–341.
[46] Takeoka, H., 1991. Water exchange and transport of matter in the Seto Inland Sea. Mar Pollut Bull 23, 41–44.
[47] Nagai, T., 2003. Recovery of fish stocks in the Seto Inland Sea. Mar Pollut Bull 47 (1–6), 126–131.
[48] Blumberg, A.F., Mellor, G.L., 1987. A description of a three-dimensional coastal ocean circulation model. Three-Dimens Coast Ocean Models 4, 1–16.
[49] Zhu, J., Guo, X., Shi, J., Gao, H., 2019. Dilution characteristics of riverine input contaminants in the Seto Inland Sea. Mar Pollut Bull 141, 91–103.
[50] Guo, X., Futamura, A., Takeoka, H., 2004. Residual currents in a semi-enclosed bay of the Seto Inland Sea, Japan. J Geophys Res: Oceans 109 (C12).
[51] Ariathurai, R., Krone, R.B., 1976. Mathematical modelling of sediment transport in estuaries. In: Wiley, M. (Ed.), Estuarine Processes, II. Academic Press, pp. 98–106.

[52] Mengual, B., Hir, P.L., Cayocca, F., Garlan, T., 2017. Modelling fine sediment dynamics: towards a common erosion law for fine sand, mud and mixtures. Water 9 (8), 564.
[53] Tessier, C., Le Hir, P., Dumas, F., Jourdin, F., 2008. Modélisation des turbidités en Bretagne sud et validation par des mesures in situ. Eur J Environ Civ Eng 12 (1-2), 179–190.
[54] Wang, X.H., 2002. Tide-induced sediment resuspension and the bottom boundary layer in an idealized estuary with a muddy bed. J Phys Oceanogr 32 (11), 3113–3131.
[55] Winterwerp, J.C., Van Kesteren, W.G., 2004. Introduction to the Physics of Cohesive Sediment Dynamics in the Marine Environment. Elsevier B.V.: Amsterdam.
[56] Waldschläger, K., Brückner, M.Z., Almroth, B.C., Hackney, C.R., Adyel, T.M., Alimi, O.S., Belontz, S.L., Cowger, W., Doyle, D., Gray, A., 2022. Learning from natural sediments to tackle microplastics challenges: a multidisciplinary perspective. Earth-Sci Rev 228, 104021.
[57] Leng, Q., Guo, X., Zhu, J., Morimoto, A., 2023. Contribution of open ocean to the nutrient and phytoplankton inventory in a semi-enclosed coastal sea. Biogeosciences 20, 4323–4338.
[58] Murawski, J., She, J., Frishfelds, V., 2022. Modeling drift and fate of microplastics in the Baltic Sea. Front Mar Sci 9, 886295.
[59] Shamskhany, A., Li, Z., Patel, P., Karimpour, S., 2021. Evidence of microplastic size impact on mobility and transport in the marine environment: a review and synthesis of recent research. Front Mar Sci 8, 760649.
[60] Chubarenko, I., Bagaev, A., Zobkov, M., Esiukova, E., 2016. On some physical and dynamical properties of microplastic particles in marine environment. Mar Pollut Bull 108 (1-2), 105–112.
[61] Pauli, N.-C., Petermann, J.S., Lott, C., Weber, M., 2017. Macrofouling communities and the degradation of plastic bags in the sea: an in situ experiment. R Soc Open Sci 4 (10), 170549.
[62] Wang, H., Guo, X., Liu, Z., 2019. The age of Yodo River water in the Seto Inland Sea. J Mar Syst 191, 24–37.
[63] Wang, G.X., Huang, D., Ji, J.H., Völker, C., Wurm, F.R., 2021. Seawater-degradable polymers—fighting the marine plastic pollution. Adv Sci 8 (1), 2001121.